Acta Mech 217, 149–155 (2011)
DOI 10.1007/s00707-010-0388-4

Yankun Feng · Yulan Liu · Biao Wang

Finite element analysis of resonant properties of silicon nanowires with consideration of surface effects

Received: 18 September 2010 / Published online: 15 October 2010

Abstract We developed a 3D finite element model taking into account the surface effects which is considered significant in nanostructures and used the model to study the resonant frequencies and Young's modulus of silicon nanowires on both fixed/fixed and fixed/free boundary conditions with diameters between 50 and 200 nm. We found that Young's modulus and resonant frequencies significantly decreased with decreasing diameter when the diameter was less than 100 nm for fixed/free boundary condition, while they slightly decreased for fixed/fixed boundary condition. When the diameter is larger than 200 nm, the surface stresses may be neglected.

1 Introduction

Nanowires have recently attracted vast interest for potential use in nanoelectromechanical systems (NEMS) and nanoelectronics [1]. The Young's modulus is of particular interest as an important parameter in the nanoscale devices such as mechanical resonators [2]. Both experiments and atomistic simulations found a size dependence of the elastic modulus of nanowires [3–7]. In particular, for silicon nanowires, when the diameter of the nanowire is less than 100 nm, the Young's modulus decreases with decreasing diameter [8].

To understand the behavior of mechanical properties of nanowires, the surface effect and surface stress may be important factors due to the high surface area-to-volume ratio in nanoscale. In classical continuum mechanics, surface energy is usually neglected. Some works, which used a linear surface constitutive equation, were done to extend the classical finite element method to analyze size-dependent mechanical properties of nanomaterials [9–11]. In this work, the total free energy will involve both bulk and surface energy contributions which are significant in nanostructure and a 3D finite element model with considering surface effects will be used to show how surface stresses influence the resonant properties of nanowires.

The following approximations are made in this work. (i) A 3D model is used to study the resonant frequencies of single crystal silicon having cross-sectional sizes ranging from 50 to 200 nm using both fixed/free and fixed/fixed boundary conditions. (ii) The linear constitutive equation between surface stress and surface strain will be used [12].

Y. Feng · Y. Liu (✉)
Department of Applied Mechanics and Engineering, Sun Yat-sen University,
135 Xingang West Road, 510275 Guangzhou, People's Republic of China
E-mail: stslyl@mail.sysu.edu.cn

B. Wang
School of Physics and Engineering, Sun Yat-Sen University,
135 Xingang West Road, 510275 Guangzhou, People's Republic of China

2 3D finite element formulation with consideration about surface stresses

According to Cammarata [13], the surface stress σ_{ij}^{s} is related to the deformation-dependent surface energy γ by Shuttleworth's equation

$$\sigma_{ij}^{s} = \gamma\delta_{ij} + \frac{\partial\gamma}{\partial\varepsilon_{ij}^{s}}, \tag{1}$$

where ε_{ij}^{s} is the surface strain, δ_{ij} is the Kronecker delta symbol. Miller et al. [12] get a linear constitutive equation

$$\sigma_{ij}^{s} = \sigma_{ij}^{0} + S_{ijkl}\varepsilon_{kl}^{s} \quad (i, j, k, l = 1, 2), \tag{2}$$

where σ_{ij}^{S} is surface stress, σ_{ij}^{0} is residual surface stress when the bulk is unrestrained, and S_{ijkl} is the surface elastic constant, and ε_{ij}^{s} is surface strain. Both S_{ijkl} and σ_{ij}^{0} can be determined from atomistic calculations. And also Eq. (2) can be rewritten to a matrix form

$$\boldsymbol{\sigma}_{\mathrm{s}} = \boldsymbol{\sigma}_{0} + \mathbf{S}\boldsymbol{\varepsilon}_{\mathrm{s}}. \tag{3}$$

The Lagrangian of the system is

$$L = T - U_{\mathrm{e}} - U_{\mathrm{s}} + W, \tag{4}$$

where T is the kinetic energy of the bulk, U_{e} and U_{s} are respectively volume elastic strain energy and surface energy. They are given by

$$T = \int_{V} \frac{1}{2}\rho\mathbf{v}^{\mathrm{T}}\mathbf{v}\mathrm{d}V \tag{5}$$

and

$$U_{\mathrm{e}} = \int_{V} \frac{1}{2}\boldsymbol{\varepsilon}^{\mathrm{T}}\mathbf{D}\boldsymbol{\varepsilon}\mathrm{d}V, \tag{6}$$

$$U_{\mathrm{s}} = \int_{\Omega} \sigma^{\mathrm{s}} d\boldsymbol{\varepsilon}^{\mathrm{s}} = \int_{\Omega} \left[\boldsymbol{\sigma}_{\mathbf{0}}\boldsymbol{\varepsilon}^{\mathrm{s}} + \frac{1}{2}\left(\varepsilon^{\mathrm{s}}\right)^{\mathrm{T}}\mathbf{S}\boldsymbol{\varepsilon}^{\mathrm{s}}\right]\mathrm{d}\Omega, \tag{7}$$

where ρ and $\mathbf{v}$ are respectively density and velocity vector, Ω denotes the domains of surface. Thus, due to Largrange's equations, we get

$$\mathbf{M}\ddot{\mathbf{u}}_{\mathrm{e}} + \left(\mathbf{K}_{\mathrm{B}} + \mathbf{K}_{\mathrm{s}}\right)\mathbf{u}_{\mathrm{e}} - \mathbf{P} + \mathbf{P}_{\mathrm{s}} = \mathbf{0}, \tag{8}$$

where $\mathbf{M}$ is the mass matrix, $\mathbf{K}_{\mathrm{B}}$ and $\mathbf{K}_{\mathrm{s}}$ are respectively classical bulk stiffness matrix and surface stiffness matrix, which is the contribution of the surface stresses, $\mathbf{P}$ and $\mathbf{P}_{\mathrm{s}}$ are respectively external force vector and residual surface stress vector, $\mathbf{u}_{\mathrm{e}}$ is the displacement vector of element nodes. The surface-energy-related terms are given as follows:

$$\mathbf{K}_{\mathrm{s}} = \int_{\Omega} \mathbf{B}_{\mathrm{s}}^{\mathrm{T}}\mathbf{S}\mathbf{B}_{\mathrm{s}}\mathrm{d}\Omega \tag{9}$$

and

$$\mathbf{P}_{\mathrm{s}} = \int_{\Omega} \mathbf{B}_{\mathrm{s}}^{\mathrm{T}}\boldsymbol{\sigma}_{0}\mathrm{d}\Omega, \tag{10}$$

where $\mathbf{B}_{\mathrm{s}}$ is the strain-displacement matrix of the surface element.

In order to calculate the surface stiffness matrix, we introduce a four-node rectangle element to describe a surface element. The displacement in the local coordinate (ξ, η, ζ) is expressed as an interpolation of the nodal displacements of local coordinates by the shape functions

$$\begin{Bmatrix} a_\xi & a_\eta & a_\zeta \end{Bmatrix}^{\mathrm{T}} = \mathbf{N}\mathbf{a}_{\mathrm{e}} \ (a_\zeta = 0), \tag{11}$$

where

$$\mathbf{N} = \begin{Bmatrix} N_1 & 0 & 0 & N_2 & 0 & 0 & N_3 & 0 & 0 & N_4 & 0 & 0 \\ 0 & N_1 & 0 & 0 & N_2 & 0 & 0 & N_3 & 0 & 0 & N_4 & 0 \end{Bmatrix} \tag{12}$$

is the shape function matrix and

$$\mathbf{a}_{\mathrm{e}} = \begin{Bmatrix} a_{\xi 1} & a_{\eta 1} & a_{\zeta 1} & a_{\xi 2} & a_{\eta 2} & a_{\zeta 2} & a_{\xi 3} & a_{\eta 3} & a_{\zeta 3} & a_{\xi 4} & a_{\eta 4} & a_{\zeta 4} \end{Bmatrix}^{\mathrm{T}} \tag{13}$$

is the nodal displacement in local coordinates. In the local coordinate system, the shape functions N_i take on the bilinear form

$$N_i = \frac{1}{4}\left(1 + \frac{\xi}{\xi_i}\right)\left(1 + \frac{\eta}{\eta_i}\right). \tag{14}$$

In order to transform the local coordinates to global coordinates, we use the relation

$$\mathbf{u}_{\mathrm{e}} = \mathbf{R}\mathbf{a}_{\mathrm{e}} \quad \text{or} \quad \mathbf{a}_{\mathrm{e}} = \mathbf{R}^{\mathbf{T}}\mathbf{u}_{\mathrm{e}}, \tag{15}$$

where $\mathbf{u}_{\mathrm{e}}$ is the displacement vector in the global coordinate system and $\mathbf{R}$ is the rotation matrix. Then, we have

$$\mathbf{B}_{\mathrm{s}} = \begin{pmatrix} \frac{\partial N_1}{\partial \xi} & 0 & 0 & \frac{\partial N_2}{\partial \xi} & 0 & 0 & \frac{\partial N_3}{\partial \xi} & 0 & 0 & \frac{\partial N_3}{\partial \xi} & 0 & 0 \\ 0 & \frac{\partial N_1}{\partial \eta} & 0 & 0 & \frac{\partial N_2}{\partial \eta} & 0 & 0 & \frac{\partial N_3}{\partial \eta} & 0 & 0 & \frac{\partial N_3}{\partial \eta} & 0 \end{pmatrix}. \tag{16}$$

The surface stiffness matrix is

$$\mathbf{K}_s = \int_{\Omega} \mathbf{R}^{\mathrm{T}}\mathbf{B}_{\mathrm{s}}^{\mathrm{T}}\mathbf{S}\mathbf{B}_{\mathrm{s}}\mathbf{R}\mathrm{d}\xi\,\mathrm{d}\eta, \tag{17}$$

and the residual surface stress vector is

$$\mathbf{P}_s = \int_{\Omega} \mathbf{R}^{\mathrm{T}}\mathbf{B}_s^{\mathrm{T}}\mathrm{d}\xi\,\mathrm{d}\eta. \tag{18}$$

To find resonant frequencies of a system, we need to solve a eigenvalue problem that is written as

$$\left(\mathbf{K} - \omega^2\mathbf{M}\right)\mathbf{u} = 0, \tag{19}$$

where in our model the stiffness matrix $\mathbf{K} = \mathbf{K}_{\mathrm{e}} + \mathbf{K}_{\mathrm{s}}$ involves the surface stress contribution.

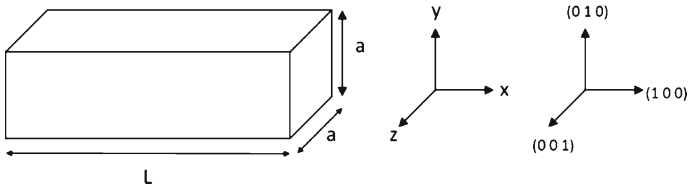

Fig. 1 Schematic diagram of a single-crystal silicon nanowire

Fig. 2 The distribution of displacement in the x-direction in the x–y plane ($z = 0$)

3 Numerical examples and discussion

All numerical examples were performed on three-dimensional, single-crystal silicon nanowires of length L that have a square cross-section of width a, and the crystallographic directions of the wires are illustrated in Fig. 1.

In this work, we will study two boundary conditions: fixed/free and fixed/fixed. The fixed/free boundary condition is fixed in the left (−x) surface of wires and free in the right (+x) surface of wires. The fixed/fixed boundary condition is fixed both in the left (−x) and right (+x) surfaces of wires. All finite element simulations were performed using the stated boundary conditions without external loading and meshing by eight-node hexahedral elements.

In order to compare the atomic simulation which has been done by Park [14], we set the model as homogeneous, the Young's modulus of silicon is chosen to be 90 GPa which is used in Park's work [14], the surface elastic properties of silicon are $S_{11} = -10.64$ N/m, $S_{12} = -3.88$ N/m, $\sigma_0 = 0.60$ N/m, [12], the geometry of the wire is $128 \times 16 \times 16$ (nm), and the boundary condition is fixed/free. The distribution of displacement in the x-direction in the x–y plane ($z = 0$) is shown in Fig 2.

The results agree with Park's work in which the author uses molecular statics calculation to study tensile expansion of the silicon nanowire [14]. In the right surface of the wire, the value of displacement in the x-direction is about 1.12 nm, and near the left surface of the wire, the value of displacement in the x-direction is about −0.06 nm. In Park's work, the value of displacement in the x-direction in the right surface and near the left surface is about 1.2 and −0.05 nm [14]. We note that the tensile strain induced in the nanowires due to the surface stresses is about 0.09%. The distribution of displacement in the x-direction also agrees with Park's work, capturing the inhomogeneous nature of the tensile expansion.

Next, we study how surface stresses affect the resonant frequencies and Young's modulus of the nanowires for different boundary conditions. The width of the section α of the chosen nanowire ranges from 50 to 200 nm and the length l constantly equals 1000 nm. The model now is set to inhomogeneous, and the elastic constant of silicon is $C_{11} = 1.009\,\text{eV} \cdot \text{Å}^{-3}$, $C_{12} = 0.5093\,\text{eV} \cdot \text{Å}^{-3}$, $C_{44} = 0.3762\,\text{eV} \cdot \text{Å}^{-3}$, and the density of silicon is $2.33\,\text{g cm}^{-3}$ [12].

In order to study the effective Young's modulus, first we will get the fundamental resonant frequencies from solving the eigenvalue problem in Eq. (19). Then, we use the well-known analytic solution of Euler–Bernoulli beams for both fixed/free and fixed/fixed boundary to calculate the effective Young's modulus of silicon nanowires. For the fixed/free beam [15]

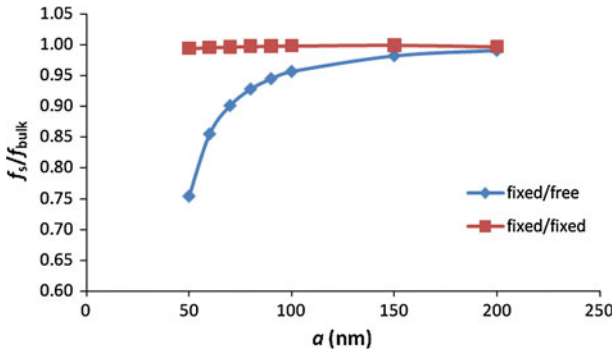

Fig. 3 Normalized resonant frequencies for constant-length silicon nanowires

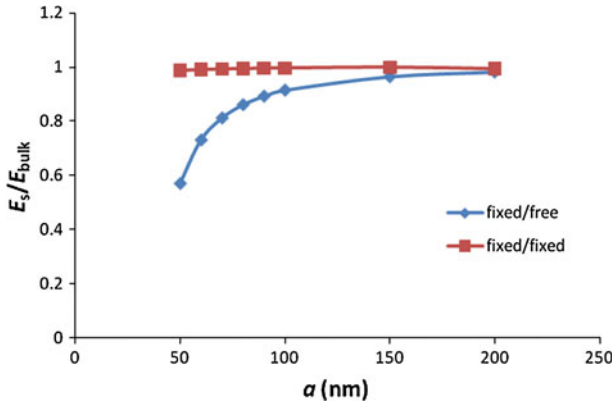

Fig. 4 Normalized Young's modulus for constant-length silicon nanowires

$$E = \frac{4\pi^2 l^4 f_0^2 \rho A}{B_0^4 I}, \tag{20}$$

where $B_0 = 1.875$ for the fundamental resonant mode, l is the nanowire's length, f_0 is the fundamental resonant frequency, ρ is the density of silicon, A is the cross-section area, and I is the moment of inertia.

For the fixed/fixed beam, the formulation is given as [15]

$$E = \frac{4l^4 f_0^2 \rho A}{i^2 \pi I}, \tag{21}$$

where $i \approx 1.5$ is a constant for fixed/fixed beams.

We plot the f_s/f_{bulk} ratio against the width a in Fig. 3, where f_s and f_{bulk} are the fundamental resonant frequencies of nanowires with consideration bulk of the surface effect and without consideration bulk of the surface effect, respectively. Figure 3 shows that for fixed/fixed boundary condition, the ratio is close to 1, which is slightly related to width a. In contrast, for fixed/free boundary condition, when the width is less than 100 nm, the frequencies decrease with decreasing width. When the width $a = 50$ nm, the resonant frequency predicted in our model is about 25% less than the bulk resonant frequency. When the width $a > 200$ nm, the ratio is close to 1.

Figure 4 shows the normalized Young's modulus plotted against the width a. The behavior of the effective Young's modulus is similar to the behavior of the resonant frequency. For fixed/fixed boundary condition, the values of the effective Young's modulus predicted in our model are close to 1 and nearly independent of width a. As can be observed, for fixed/free boundary condition, the normalized Young's modulus predicted in our model decreases with decreasing width a. When the width $a = 50$ nm, the value of the effective Young's modulus is about 43% lower than the bulk value. When the width $a > 200$ nm, the value of the effective Young's modulus in our model approximately equals the bulk value. In our calculation, (i) $a <$ 100 nm, there is strong size dependence of resonant frequency and Young's modulus for fixed/free nanowires.

Table 1 The value of normalized frequencies and normalized Young's modulus

Width a (nm)	Fixed/free		Fixed/fixed	
	f_s/f_{bulk}	E_s/E_{bulk}	f_s/f_{bulk}	E_s/E_{bulk}
200	0.990	0.980	0.997	0.993
150	0.981	0.963	0.999	0.998
100	0.956	0.913	0.998	0.996
90	0.944	0.891	0.997	0.995
80	0.927	0.859	0.997	0.994
70	0.900	0.810	0.996	0.992
60	0.854	0.729	0.995	0.990
50	0.754	0.569	0.993	0.987

(ii) $a > 200$ nm, for both fixed/free and fixed/fixed nanowires, there is a very small variation of resonant frequency and Young's modulus. So in this case, surface stresses may be neglected.

Table 1 lists the values of the normalized frequencies and normalized Young's modulus for both fixed/free and fixed/fixed boundary conditions. As can be observed, both normalized frequencies and normalized Young's modulus decrease slightly with decreasing width a for fixed/fixed boundary conditions. When the width $a = 50$ nm, for fixed/fixed nanowires, the value of the effective Young's modulus is about 2% lower than the bulk value and the value of the resonant frequency is about 1% lower than the bulk value.

Different behaviors of the Young's modulus of nanowires is observed in experiments on different boundary conditions. The work of Li et al. shows that the Young's modulus of nano silicon cantilevers (fixed/free) decreases with decreasing diameter and the value of Young's modulus is about 59% lower than the bulk value [5]. And Jing et al. shows that for fixed/fixed silver nanowires, experimental data show little variation of bulk Young's modulus when the diameters of nanowires are larger than 50 nm [16]. We consider that it is similar for silicon nanowires. Jin et al. introduced the surface stress into Euler–Bernoulli beam theory, and their results also find that different boundary conditions have different effects on the Young's modulus of nanowires [17].

Our present results agree with the available experimental data [5,16] and theoretical results [17] in prediction of a relative decrease in Young's modulus for fixed/free nanowires and a little variation in Young's modulus for fixed/fixed nanowires.

4 Conclusion

In conclusion, we incorporate surface effects into a conventional finite element method and develop a 3D finite element model of nanomaterials. It is an attempt to extend the classical FEM approach to analyze nanomaterials. Analysis of mechanical properties of silicon nanowires for two boundary conditions is given to demonstrate the surface effects on the frequencies and effective Young's modulus. We find that Young's modulus and resonant frequencies decrease for fixed/free nanowires and have little variation for fixed/fixed nanowires. When the diameter is larger than 200 nm, surface stresses may be neglected.

Acknowledgments The project is supported by the National Natural Science Foundation of China (10972239, 10732100, 11072271)

References

1. Craighead, H.G.: Nanoelectromechanical systems. Science **290**, 1532–1535 (2000)
2. Feng, X.L., He, R.R., Yang, P.D., Roukes, M.L.: Very high frequency silicon nanowire electromechanical resonators. Nano Lett. **7**, 1953–1959 (2007)
3. Cuenot, S., Fretigny, C., Demoustier-Champagne, S., Nysten, B.: Surface tension effect on the mechanical properties of nanomaterials measured by atomic force microscopy. Phys. Rev. B **69**, 165410 (2004)
4. Broughton, J.Q., Meli, C.A., Vashishta, P., Kalia, R.K.: Direct atomistic simulation of quartz crystal oscillators: Bulk properties and nanoscale devices. Phys. Rev. B **56**, 611–618 (1997)
5. Li, X.X., Ono, T., Wang, Y.L., Esashi, M.: Ultrathin single-crystalline-silicon cantilever resonators: Fabrication technology and significant specimen size effect on Young's modulus. Appl. Phys. Lett. **83**, 3081–3083 (2003)
6. Wang, G.F., Li, X.D.: Size dependency of the elastic modulus of ZnO nanowires: Surface stress effect. Appl. Phys. Lett. **91**, 231912 (2007)

7. Lee, B., Rudd, R.E.: First-principles study of the Young's modulus of Si <001> nanowires. Phys. Rev. B **75**, 041305 (2007)
8. Zhu, Y., Xu, F., Qin, Q.Q., Fung, W.Y., Lu, W.: Mechanical properties of vapor-liquid-solid synthesized silicon nanowires. Nano Lett. **9**, 3934–3939 (2009)
9. She, H., Wang, B.: Finite element analysis of conical, dome and truncated InAs quantum dots with consideration of surface effects. Semicond. Sci. Tech. **24**, 4 (2009)
10. She, H., Wang, B.A.: A geometrically nonlinear finite element model of nanomaterials with consideration of surface effects. Finite. Elem. Anal. Des. **45**, 463–467 (2009)
11. Gao, W., Yu, S.W., Huang, G.Y.: Finite element characterization of the size-dependent mechanical behaviour in nanosystems. Nanotechnology **17**, 1118–1122 (2006)
12. Miller, R.E., Shenoy, V.B.: Size-dependent elastic properties of nanosized structural elements. Nanotechnology **11**, 139 (2000)
13. Cammarata, R.C.: Surface and interface stress effects in thin-films. Prog. Surf. Sci. **46**, 1–38 (1994)
14. Park, H.S.: Surface stress effects on the resonant properties of silicon nanowires. J. Appl. Phys. **103**, 123504 (2008)
15. Weaver, W., Timoshenko, S., Young, D.: Vibration Problems in Engineering. Wiley-Interscience, New York (1990)
16. Jing, G.Y., Duan, H.L., Sun, X.M., Zhang, Z.S., Xu, J., Li, Y.D., Wang, J.X., Yu, D.P.: Surface effects on elastic properties of silver nanowires: Contact atomic-force microscopy. Phys. Rev. B **73**, 235049 (2006)
17. He, J., Lilley, C.M.: Surface stress effect on bending resonance of nanowires with different boundary conditions. Appl. Phys. Lett. **93**, 263108 (2008)